

Vortex pinning behaviour in MgB₂ bulk samples obtained by electric-field assisted sintering

L. MIU, I. IVAN, G. ALDICA, P. BADICA, J. R. GROZA^a, D. MIU^b, G. JAKOB^c, H. ADRIAN^c

National Institute of Materials Physics, 77125 Bucharest-Magurele, P. O. Box MG-7, Romania

^a*Department of Chemical Engineering and Materials Science, University of California, Davis, 95616-5294 California, USA*

^b*National Institute for Laser, Plasma, and Radiation Physics, 77125 Bucharest-Magurele, P. O. Box MG-36, Romania*

^c*Institute of Physics, University of Mainz, 55128 Mainz, Germany*

Well-compacted MgB₂ specimens with the density higher than 90 % of the theoretical value were obtained by electric-field assisted sintering. This method assures a good grain connectivity, which leads to the appearance of efficient pinning centres at the grain boundaries. We measured the DC magnetization curves and the relaxation of the irreversible magnetization using the SQUID magnetometry for a magnetic field H up to 50 kOe applied in zero-field-cooling conditions. The critical current density is of the order of 10^{10} A/m² at $H = 20$ kOe and $T = 10$ K. A crossover plastic creep at high temperatures T – elastic creep at low T described by $H \propto T^{-2}$ in the low T – high H domain was observed. This is caused by the macroscopic currents induced in the sample during magnetization measurements. By decreasing T below this line the determined creep exponent rapidly overcomes the widely accepted theoretical values for elastic (collective) pinning. This behaviour can be explained through the occurrence of micro flux jumps, which seem to be responsible for the finite magnetization relaxation rate in the low- T limit. The relaxation of the irreversible magnetization allowed us the precise determination of the characteristic pinning energy barrier.

(Received September 1, 2008; accepted October 30, 2008)

Keywords: Superconductors, MgB₂, Electric-field assisted sintering, Vortex pinning, Magnetization relaxation

1. Introduction

The absence of weak-link behaviour in MgB₂ together with a relatively high critical temperature T_c [1] opened up the possibility of a new class of low-cost – high-performance superconducting materials. One important issue is to attain competitive values for the critical current density J_c , which is controlled by the vortex mobility – pinning relation. Vortex pinning in MgB₂ single crystals is weak, which is not the case for well compacted polycrystalline specimens and thin films [2]. While J_c values approaching the pair breaking limit were found in thin films at low H [3], a δT_c pinning with a small bundle collective (elastic) pinning in a large portion of the vortex phase diagram was proposed for bulk samples in Ref. [4]. It was also reported that for $H < 8$ kOe a (dislocation free) Bragg-glass state [5] exists in well compacted samples obtained by hot isostatic pressing [6], whereas a grain boundary pinning [where the pinning behaviour of bulk specimens is described by the traditional (plastic) flux-shear mechanism] was discussed in Refs. [7,8]. The experimental investigation of the pinning mechanism in MgB₂ is often based on the H dependence of the normalized pinning force, with the latter extracted from the DC magnetization curves [9].

An essential tool for the study of vortex dynamics in the presence of pinning is the relaxation of the irreversible magnetization. It was shown [10] that the irreversible magnetization of MgB₂ bulk samples depends

logarithmically of time, i. e., the flux-creep activation energy would decrease linearly with increasing current density J , as expected in the framework of the Kim-Anderson model [11]. On the other hand, AC susceptibility measurements performed on similar specimens [12] revealed the fact that the flux-creep activation energy is a nonlinear function of J . The relaxation of the irreversible magnetization in the low- T domain suggests that the flux dynamics in MgB₂ may be dominated by quantum effects [13,14], such as quantum fluctuations and tunnelling, but the magnetization measured at low T is affected by flux jumps or avalanches [15]. Further investigations are needed to clarify these aspects.

In this work we analyze the DC magnetization curves and the relaxation of the irreversible magnetization of compact MgB₂ bulk samples prepared by electric-field assisted sintering. J_c values of the order of 10^{10} A/m² at $H = 20$ kOe and for $T = 10$ K were attained. We found a large influence of the macroscopic currents induced in the sample during experiments, leading to a crossover plastic creep at high T – elastic creep at low T , similar to that observed for Bi₂Sr₂CaCu₂O_{8 + δ} single crystals [16] and YBa₂Cu₃O_{7 - δ} films [17]. However, by decreasing T below the creep-crossover line the determined creep exponent rapidly overcomes the widely accepted theoretical values for elastic (collective) pinning, signalling the presence of micro flux jumps. We suggest that the anomalous behaviour of the magnetization

relaxation rate at low T can be caused by the occurrence of micro flux jumps.

2. Experimental

MgB₂ bulk samples with the density higher than 90% of the theoretical value were obtained by electric-field assisted sintering. The main characteristic of this technique is that a pulsed DC current directly passes through the conductive powder compact. The heat is generated internally, in contrast to the conventional hot pressing, where the heat is provided by external heating elements. This method is currently used to consolidate ceramic, metal and composite powders. Preparation details and the microstructure of the specimens investigated in this work can be found in Ref. [18]. The characteristic sample dimensions were $\sim 1 \times 1 \times 0.4$ mm³, with the largest side perpendicular to the direction along which the pressure was applied during the sintering process.

The magnetization M was measured using a commercial Quantum Design MPMS in the RSO mode, with H applied in zero-field-cooling conditions and oriented perpendicular to the largest sample side. The onset of the diamagnetic signal for $H = 10$ Oe occurs at the critical temperature $T_c \sim 38.5$ K, and the transition width is ~ 1 K. In the (H, T) domain considered below M was identified with the irreversible magnetization, and the magnetization relaxation measurements were performed with the magnet in the persistent mode. The relaxation time t was taken to be zero when magnet charging was finished, and the first data point was registered at $t_1 \sim 100$ s.

3. Results and discussions

Fig. 1 (main panel) illustrates the DC magnetization curves $M(H)$ obtained with the magnet in the hysteresis mode for T between 2 K and 28 K. One can see the presence of macroscopic flux jumps [19] at $T = 2$ K and 5 K for H below ~ 20 kOe. J_c determined with the Bean model [20] using the data from the main panel of Fig. 1 is plotted vs. H in Fig. 2. The inset to Fig. 1 shows $|M|$ vs. $\ln(t)$ for $H = 30$ kOe and several T values (where no macroscopic jumps on the DC magnetization curves are seen in our measurements), which would suggest that M relaxes logarithmically in time, in agreement with the Kim-Anderson model [11].

As known, in the framework of this approach the vortex-creep activation energy $U(J) = U_0(1 - J/J_c)$, where the barrier U_0 can depend on H and T . The above $U(J)$ form leads to a logarithmic $M(t)$ variation, $M(t) = M(t_0)[1 - (T/U_0)\ln(t/t_0)]$, where $|M| \propto J$ and t_0 is the macroscopic time scale for creep or the vortex hopping ‘‘attempt’’ time [21].

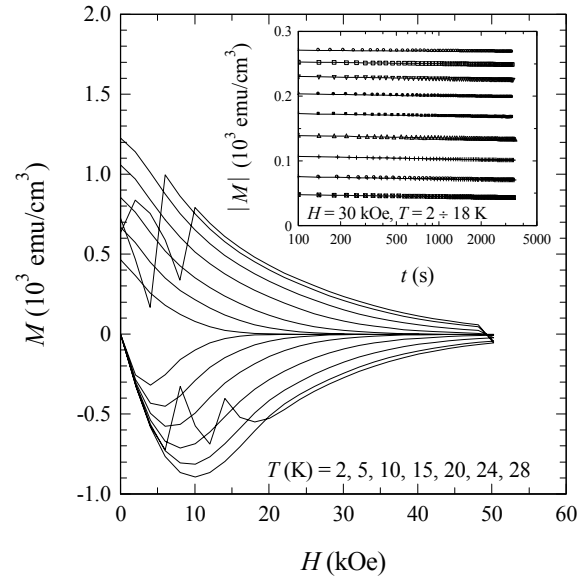


Fig. 1. Main panel: DC magnetization curves $M(H)$ of compact MgB₂ bulk samples for several T values between 2 K and 28 K, obtained with the magnet in the hysteresis mode and the step $\Delta H = 2$ kOe. For $T = 2$ K and 5 K and H below ~ 20 kOe macroscopic flux jumps are present. The inset illustrates the absolute value of the magnetization $|M|$ vs. $\ln(t)$ for $H = 30$ kOe and T between 2 K and 18 K (with the step in T of 2 K). The weak magnetization relaxation and the usually small relaxation time window are responsible for the fact that $M(t)$ appears to be linear in $\ln(t)$.

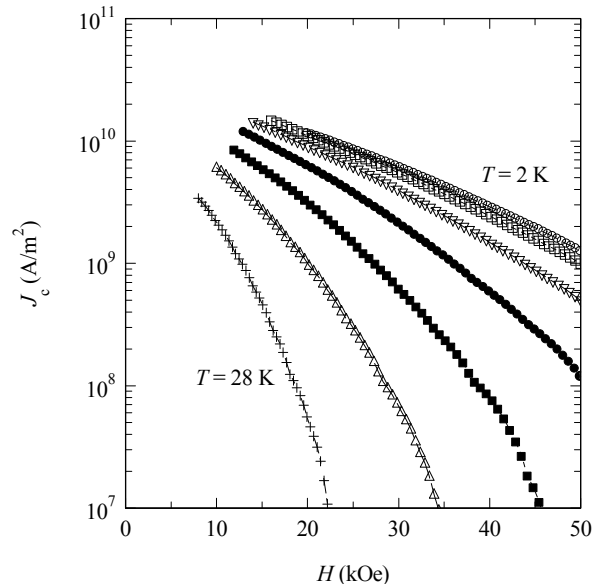


Fig. 2. Critical current density J_c vs. T determined with the Bean model [20] from the data shown in the main panel of Fig. 1. The whole sample screening was assumed.

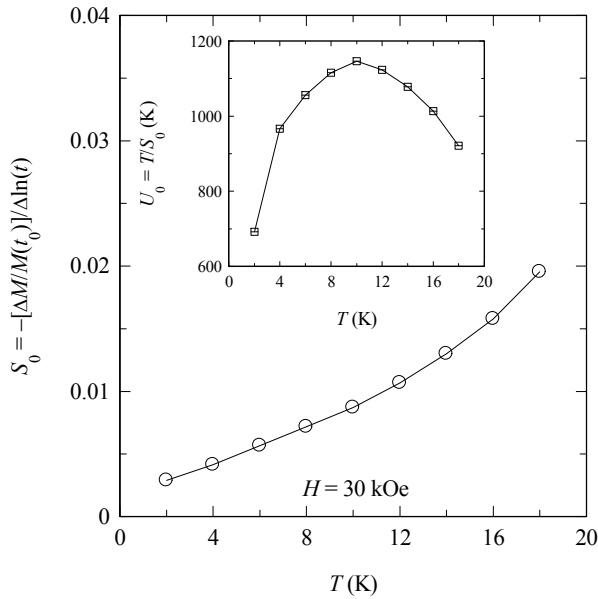


Fig. 3. Main panel: T variation of the magnetization relaxation rate $S_0 = -[\Delta M/M(t_0)]/\Delta \ln(t)$ determined using the magnetization relaxation data from the inset to Fig. 1 [with $M(t_0) = M(10^{-3}$ s), obtained by extrapolation]. The resulting pinning barrier $U_0(T) = T/S_0$ is plotted in the inset.

In the linear $U(J)$ model [11] the relaxation data from the inset to Fig. 1 allows the determination of the magnetization relaxation rate [22] $S_0 = -[\Delta M/M(t_0)]/\Delta \ln(t) = T/U_0$.

Fig. 3 (main panel) shows the $S_0(T)$ dependence for $H = 30$ kOe with $M(t_0) = M(10^{-3}$ s) obtained by extrapolation, whereas the resulting $U_0(T) = T/S_0$ is plotted in the inset. The decrease of $U_0(T)$ with decreasing T in the low- T domain (see the inset to Fig. 3) is unnatural, since at low T the characteristic superconducting lengths have a slow variation with T , and U_0 should not change significantly with T . (At this point, it is worthy to note that for H above ~ 10 kOe the contribution of the π band to the superelectron density is negligible [2].) The nonmonotonous $U_0(T)$ variation appears for every plausible t_0 value, including the microscopic vortex hopping attempt time, of the order of $10^{-11} \div 10^{-10}$ s [21].

In order to reduce the recognized intrinsic ambiguity of flux-creep experiments [related to $M(t_0)$, for example], it is better to analyze the J dependence of the normalized vortex-creep activation energy $U^* = -T\Delta \ln(t)/\Delta \ln(|M|)$ [22]. [For a limited relaxation time window and a weak $M(t)$ variation, the instantaneous $U^*(J) = -T d \ln(t)/d \ln(|M|)$ extracted from a single magnetization relaxation curve is highly affected by the measurement sensitivity and the error in setting the moment $t = 0$.] Plotting $\ln|M(t)|$ vs. $\ln(t)$ the (almost) linear variation is preserved, and we determined a normalized magnetization relaxation rate $S = -\Delta \ln(|M|)/\Delta \ln(t)$ averaged over the whole relaxation time window, as well as the normalized vortex-creep activation energy $U^* = T/S$.

The $S(T)$ variation for several H values is illustrated in the main panel of Fig. 4, whereas the resulting $U^*(T)$ dependence is shown in the inset. As can be seen in the main panel, $S(T)$ does not extrapolates to zero when $T \rightarrow 0$, which would be a reason to invoke a large contribution of vortex tunnelling in MgB₂. The notable feature in the inset to Fig. 4 is the appearance of a maximum in $U^*(T)$, similar to the $U_0(T)$ variation from Fig. 3. This indicates that the observed $U^*(T)$ or $U_0(T)$ maximum is not caused by the variation of t_0 with T , but is generated by a nonlinear $U(J)$ [23], as shown below. The weak $M(t)$ variation and the usually small relaxation time window are responsible for the fact that the magnetization relaxation from the inset to Fig. 1 appears to be logarithmic in time.

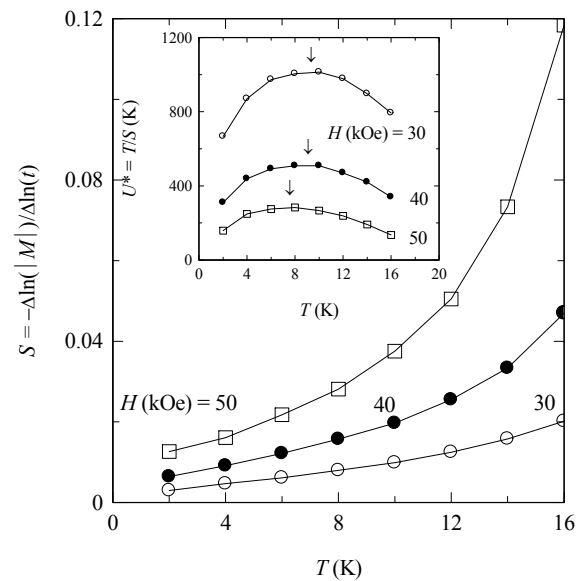


Fig. 4. T variation of the normalized magnetization relaxation rate $S = -\Delta \ln(|M|)/\Delta \ln(t)$ averaged over the relaxation time window for several H values (main panel), and the corresponding normalized vortex-creep activation energy $U^*(T) = T/S$ (inset). A maximum in $U^*(T)$ appears (indicated by an arrow), which shifts to lower T values with increasing H .

The meaning of U^* appears if one uses the parameterization of the actual vortex-creep activation energy U from Ref. [24]:

$$U(T, H, J) = (U_c / p) [(J_c / J)^p - 1], \quad (1)$$

where U_c is the characteristic pinning energy, whereas the exponent p is identified with the (positive) collective pinning exponent μ in the case of elastic (collective) creep [25], and $p < 0$ for plastic vortex creep, with $p = -1$ reproducing the linear model [11]. In a crude approximation, for a given H we will neglect the T variation of J_c , U_c , and p at low T .

It was argued in Ref. [16] that the nonmonotonous $U^*(T)$ at low T actually results from a crossover in the creep process induced by the macroscopic currents in the

sample. In the low- T range, where the pinning potential is practically independent of T , the main role of the thermal energy is to change the J interval probed in standard magnetization relaxation measurements. [This is due to a different (T dependent) overall relaxation in the time interval between the moment when the magnet charging was finished ($t \approx 0$) and the time t_1 at which the first data point was taken.] When J increases the effective pinning decreases, and the elastic energy in the vortex system can overcome the effective pinning energy. In this situation, not only vortices [25] but even the dislocations will be collectively (elastically) pinned [26]. With Eq. (1) for U and keeping $J (\propto |M|)$ as explicit variable, one can derive $U^*(J)$ [17] using the general creep relation $U = T \ln(t/t_0)$ [27]. For the elastic creep domain it results

$$U^*(J) = U_c (J_c / J)^\mu, \quad (2)$$

where $\mu > 0$, and U^* will decrease with increasing J . In the plastic creep regime, for T above the maximum in $U^*(T)$, besides the intrinsic decrease of the pinning potential with increasing T the decrease of U^* with decreasing J (increasing T) arises from

$$U^* \propto (J / J_c)^{|p|}. \quad (3)$$

Plotted vs. J (extracted with the Bean model [20] assuming whole sample screening), U^* from the inset to Fig. 4 exhibits indeed a maximum.

An evidence for the interpretation of the $U^*(J)$ maximum from the main panel of Fig. 5 in terms of a current-induced crossover plastic creep at low J – elastic creep at high J comes from the form of the crossover line in the (H, T) plane, which is similar to that observed for Bi₂Sr₂CaCu₂O_{8+ δ} single crystals and YBa₂Cu₃O_{7- δ} films [16,17]. In the inset to Fig. 5 we plotted the determined T values for the $U^*(T)$ maximum (like those from the inset to Fig. 4) vs. H (log-log scales) for two similar MgB₂ samples. For standard DC magnetic measurements the current-induced creep crossover line at low T is close to the form

$$H = aT^{-2}, \quad (4)$$

where $a \approx 3 \cdot 10^3$ kOeK² in the case of our MgB₂ specimens. The above relation can be derived [16] by considering that for the J value at the $U^*(J)$ maximum the effective pinning energy equals the elastic energy in the vortex system $E_{el} \propto H^{-1/2}$ [21]. This corresponds to the energy balance equation for the static order-disorder transition induced by the quenched disorder [29], where the static pinning energy is substituted by the J -dependent effective pinning energy. Roughly, the latter is proportional to U , and for T well below T_c and a limited relaxation time window $U \propto T$ (neglecting the variation of t_0), which immediately leads to Eq. (4).

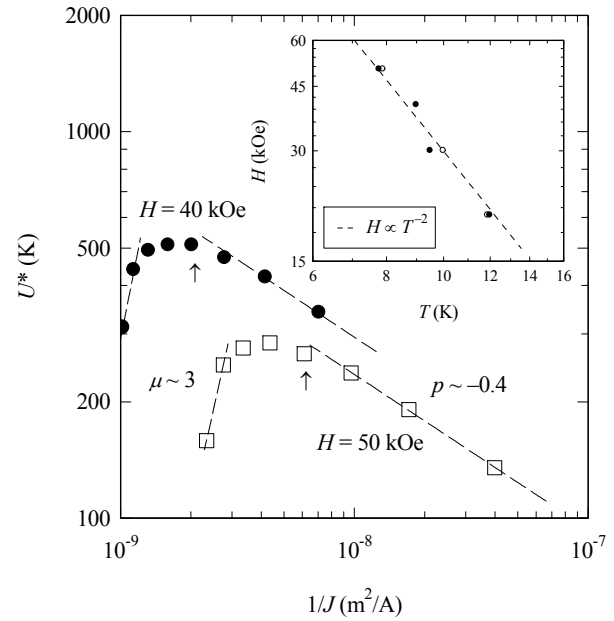


Fig. 5. Main panel: The normalized vortex-creep activation energy U^* vs. $1/J$ (double logarithmic plot) in the low- T range for $H = 40$ kOe and 50 kOe. Here J is the density of the macroscopic currents induced in the sample, and the maximum in U^* reveals a current-induced crossover plastic vortex creep at low J – elastic creep at high J . The large exponent at high J ($\mu \sim 3$, dotted lines) signals the presence of micro flux jumps, whereas the observed plastic exponent $p \sim -0.4$ (dotted lines) is close to the value proposed in Ref. [28] $p = -0.5$). The arrows indicate $T = 10$ K. The inset shows the determined T values for the $U^*(T)$ maximum (like those from the inset to Fig. 4) vs. H (log-log scales) for two similar MgB₂ samples. For standard DC magnetic measurements at low T the current-induced creep crossover line is of the form $H \propto T^{-2}$ (dotted line), similar to that observed for Bi₂Sr₂CaCu₂O_{8+ δ} single crystals and YBa₂Cu₃O_{7- δ} films [16,17].

As shown above, the normalized vortex-creep activation energy U^* is very useful for detecting changes in the vortex-creep process, but U^* actually differs from the effective pinning energy [identified with U in Eq. (1)]. However, it is easy to show that at the crossover elastic creep – plastic creep, corresponding to the $U^*(T)$ maximum from the inset to Fig. 4 [or, equivalently, to the $U^*(J)$ maximum from the main panel of Fig. 5], one has $U^* = U_c$. This is because at the creep-crossover line, where the creep exponent changes sign, U takes the form

$$U(J) = U_c \ln(J_c / J). \quad (5)$$

Neglecting the $U_c(T)$ variation for T well below T_c , a few values of the characteristic pinning energy at the creep-crossover line are plotted in Fig. 6.

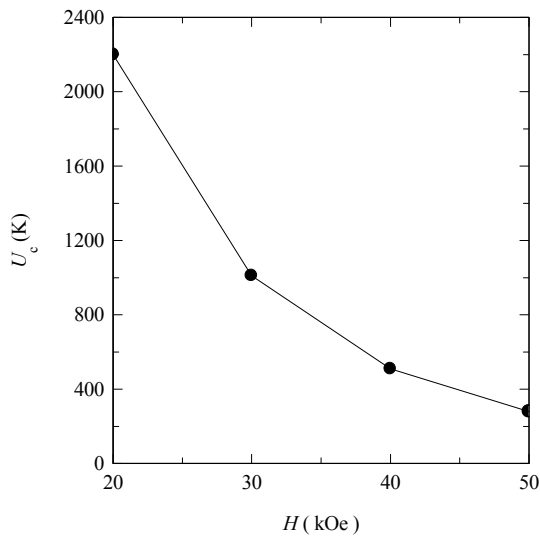


Fig. 6. The characteristic pinning energy U_c determined at the creep-crossover line vs. H for our MgB_2 bulk samples obtained by electric-field assisted sintering.

4. Conclusions

In summary, we investigated the relaxation of the irreversible magnetization in MgB_2 bulk samples compacted by electric-field assisted sintering. We observed a current-induced crossover plastic creep at high T – elastic creep at low T , similar to that appearing for $Bi_2Sr_2CaCu_2O_{8+\delta}$ single crystals and $YBa_2Cu_3O_{7-\delta}$ films. In the case of standard DC magnetization measurements this crossover is described by $H \propto T^{-2}$ in the low- T – high- H region of the vortex phase diagram, and explains why the vortex creep appears to be elastic in some experiments and plastic in others. By decreasing T below this line the exponent resulting from the current density dependence of the normalized vortex-creep activation energy rapidly overcomes the widely accepted values for a collective creep exponent. This indicates the presence of micro flux jumps, which set in by decreasing T in the elastic creep regime. The occurrence of micro flux jumps seems to be the cause for the observed finite magnetization relaxation rate in the low- T limit.

References

[1] J. Nagamatsu, N. Nakagawa, T. Muranaka, Y. Zenitani, J. Akimitsu, *Nature (London)* **410**, 63 (2001).
 [2] M. Eisterer, *Supercond. Sci. Technol.* **20**, R47 (2007), and references therein.
 [3] M. N. Kunchur, S. -I. Lee, W. N. Kang, *Phys. Rev. B* **68**, 064516 (2003).
 [4] M. J. Qin, X. L. Wang, H.K. Liu, S.X. Dou, *Phys. Rev. B* **65**, 132508 (2002).
 [5] T. Giamarchi, P. Le Doussal, *Phys. Rev. B* **55**, 6577 (1997).

[6] M. B. Maple, B. J. Taylor, S. Li, N. A. Frederick, V. F. Nesterenko, S. S. Indrakanti, *Physica C* **387**, 131 (2003).
 [7] M. Eisterer, M. Zehetmayer, H.W. Weber, *Phys. Rev. Lett.* **90**, 247002 (2003).
 [8] E. Martínez, P. Mikheenko, M. Martínez-López, A. Millán, A. Bevan, J.S. Abell, *Phys. Rev. B* **75**, 134515 (2007).
 [9] J. L. Wang, R. Zeng, J. H. Kim, L. Lu, S. X. Dou, *Phys. Rev. B* **77**, 174501 (2008).
 [10] H. Jin, H.H. Wen, H.P. Yang, Z.-Y. Liu, Z.-A. Ren, G.-C. Che, Z.-X. Zhao, *Appl. Phys. Lett.* **83**, 2626 (2003).
 [11] P. W. Anderson, Y. B. Kim, *Rev. Mod. Phys.* **36**, 39 (1964).
 [12] M. J. Qin, X. L. Wang, S. Soltanian, A. H. Li, H. K. Liu, S. X. Dou, *Phys. Rev. B* **64**, 060505(R) (2001).
 [13] H. H. Wen, S. L. Li, Z. W. Zhao, Y. M. Ni, W. N. Kang, H.-J. Kim, E.-M. Choi, S.-I. Lee, *Phys. Rev. B* **64**, 134505 (2001).
 [14] D. Zola, M. Polichetti, M. G. Adesso, L. Martini, S. Pace, *Physica C* **460-462**, 795 (2007).
 [15] J. Albrecht, A.T. Matveev, J. Stremper, H. -U. Habermeier, D. V. Shantsev, Y. M. Galperin, T. H. Johansen, *Phys. Rev. Lett.* **98**, 117001 (2007).
 [16] L. Miu, *Phys. Rev. B* **72**, 132502 (2005).
 [17] L. Miu, *Physica C* **468**, 1254 (2008).
 [18] V. Sandu, G. Aldica, P. Badica, J. R. Groza, P. Nita, *Supercond. Sci. Technol.* **20**, 1 (2007).
 [19] Å. A. F. Olsen, T. H. Johansen, D. Shantsev, E.-M. Choi, H.-S. Lee, H. J. Kim, S.-I. Lee, *Phys. Rev. B* **76**, 024510 (2007).
 [20] C. P. Bean, *Phys. Rev. Lett.* **8**, 250 (1962).
 [21] G. Blatter, M. G. Feigel'man, V. B. Geshkenbein, A. I. Larkin, V.M. Vinokur, *Rev. Mod. Phys.* **66**, 1125 (1994), and references therein.
 [22] Y. Yeshurun, A. P. Malozemoff, A. Shaulov, *Rev. Mod. Phys.* **68**, 911 (1996).
 [23] W. A. Fietz, W. W. Webb, *Phys. Rev.* **178**, 657 (1969).
 [24] A. P. Malozemoff, *Physica C* **185-189**, 264 (1991).
 [25] M. V. Feigel'man, V. B. Geshkenbein, A. I. Larkin, V. M. Vinokur, *Phys. Rev. Lett.* **63**, 2303 (1989).
 [26] J. Kierfeld, V. Vinokur, *Phys. Rev. B* **61**, R14928 (2000).
 [27] V. B. Geshkenbein, A. I. Larkin, *Sov. Phys. JETP* **60**, 639 (1989).
 [28] Y. Abulafia, A. Shaulov, Y. Wolfus, R. Prozorov, L. Burlachkov, Y. Yeshurun, D. Majer, E. Zeldov, H. Wühl, V. B. Geshkenbein, V. M. Vinokur, *Phys. Rev. Lett.* **77**, 1596 (1996).
 [29] V. Vinokur, B. Khaykovich, E. Zeldov, M. Konczykowski, R.A. Doyle, P. Kes, *Physica C* **295**, 209 (1998).

*Corresponding author: elmiu@infim.ro

